Harmonic State-Space Model of Second-Order Generalized Integrator Phase-Locked Loop

Ratik Mittal, *Student Member, IEEE,* Lingling Fan, *Senior Member, IEEE*, Zhixin Miao, *Senior Member, IEEE*

***Abstract*—Single-Phase Phase-Locked Loop (PLL) are widely used for integrating single-phase power converters. Over the years, many models for single-phase PLLs have been developed. One such PLL is Second-Order Generalized Integrator (SOGI)- PLL, which is a quadrature signal generator-based PLL. The modeling of these kinds PLLs is usually done using traditional Linear Time-Invariant (LTI) approach, which only considers fundamental frequency in the system, ignoring other higher frequencies. In this paper, Linear Time-Periodic (LTP) framework is utilized for modeling SOGI-PLL to obtain a more accurate picture of the system. First, from the nonlinear model of the PLL, a LTP model is derived. Next, using the harmonic balance method, a LTI harmonic state-space model is obtained. The two models obtained are then simulated and validated with the nonlinear model in MATLAB/Simulink. In addition to time-domain simulation, frequency-domain responses from the LTI model and the nonlinear model are compared for validation. While the frequency-domain response of the LTI model can be obtained by plotting the Bode plots of an input-output transfer function, the frequency-domain response of the nonlinear model is obtained using the harmonic injection method.**

***Index Terms*—Harmonic State-Space Model, linear time-invariant (LTI) systems, linear time-periodic (LTP) systems, phase-locked loop (PLL)**

I. Introduction

SINGLE-phase power converters have received a lot of attention for integrating small-scale renewable energy sources. Synchronization of such power converters is done using single-phase PLL. Over the years, different single-phase PLL structures have been developed and studied. The two broad categories of single-phase PLL are: i) pPLLs (power based) and, ii) quadrature signal generator (QSG)-based PLL [1], [2], [3] and, [4]. Generally, the modeling of these single-phase PLLs was done using the traditional LTI modeling methods, e.g., [5], [6]. In [5], the LTI modeling of SOGI-PLL and Park-PLL is presented. [6] presents the linearized small-signal model of fixed frequency SOGI-PLL.The traditional LTI modeling approach assumes that the system only contains fundamental frequency, ignoring the higher-frequency terms. This assumption is not valid since a frequency drift can cause second-harmonic ripples [6]; thus, the assumption may not provide the accurate picture of the system in consideration. To overcome these drawbacks, the LTP modeling framework has been widely adopted, which was introduced by Werely [7] back in 1991. Unlike traditional LTI modeling approach, LTP modeling framework performs the linearization process around a steady-state operating periodic trajectory.

R.Mittal, L.Fan and Z.Miao are with the Department of Electrical Engineering, University of South Florida, Tampa, FL, 33630 USA. Email: linglingfan@usf.edu

In [8], Orillaza has used the LTP theory to model a three-phase thyristor controlled reactor (TCR) in voltage control mode, including the control systems. Golestan in [9], has modeled SOGI-frequency-locked loop and enhanced PLL (EPLL) using the LTP theory and compared the results with the conventional LTI modeling approach. It is found that the LTP modeling approach leads to more a more accurate model.

In this paper, the focus is SOGI-PLL, which was introduced in [10]. First, from the nonlinear model of SOGI-PLL, a LTP model is obtained by linearizing the system at a steady-state periodic trajectory, or harmonic linearization. Then, using the harmonic balance method, a LTI model or a harmonic state-space model is derived. The LTI model is obtained for some relevant harmonics, to keep the system less complex. The outputs from the LTP model are time-domain signals, while the outputs from the LTI model are complex Fourier coefficients of these time-domain signals. From the complex Fourier coefficients, the time domain signals can be reconstructed. The two models obtained are subsequently simulated, and benchmarked with the original nonlinear model. Finally, the harmonic injection method is used to extract the input-output transfer function from the nonlinear model. The LTI model is also used to obtain the input-output transfer function. Bode plots of the two transfer functions obtained are presented for validation.

The contribution of this paper is two-fold.

- A harmonic state-space model of a single-phase SOGI-PLL is derived and validated using both time-domain and frequency-domain data.
- A modular LTP model derivation procedure is offered in this paper. The proposed procedure leads to module by module small-scale LTP modules. An LTP model can be found by integrating the modules. This derivation procedure is more efficient.

Fig. 1 illustrates the modeling process adopted in this paper.

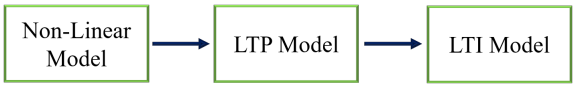

Fig. 1: Modeling process adopted for the SOGI-PLL.

The rest of the paper is organized as follows. Section II is a brief introduction of the SOGI-PLL. Section III illustrates the LTP modeling of the PLL. Section IV establishes the LTI model of the PLL. Section V demonstrates the simulation results for the two models obtained and their validation with

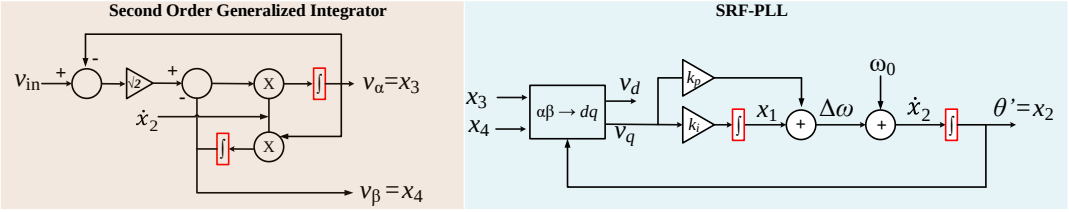

Fig. 2: Block diagram of the standard SOGI-PLL.

nonlinear model of the PLL, in MATLAB/Simulink. Section VI concludes the paper.

II. SOGI-PLL

The block diagram of the SOGI-PLL is shown in Fig. 2.

The SOGI-PLL has two parts, a) SOGI b) Synchronous Reference Frame (SRF) PLL. The single-phase input to the PLL is given by:

$$v_{in}(t) = \hat{V}\sin(\omega_0\, t) \tag{1}$$

where $\hat{V}$ (=1 $p.u$) is the magnitude and ω_0 is the fundamental frequency of $2\pi 60$ rad/s.

The output of SOGI part of the PLL are two sine waves, one with the same magnitude and initial phase angle as the input $v_{in}(t)$, and second with a phase shift of 90°. The input to the SRF-PLL are these two sine signals, $v_\alpha(t)$ and $v_\beta(t)$. The SRF-PLL consists of a Park's transformation block (2) ($\alpha\beta \rightarrow dq$) and a PI controller.

$$\begin{bmatrix} v_{dq} \end{bmatrix} = \begin{bmatrix} \sin\theta' & -\cos\theta' \\ \cos\theta' & \sin\theta' \end{bmatrix} \begin{bmatrix} v_{\alpha\,\beta} \end{bmatrix} \tag{2}$$

III. LTP Modeling

The input signal to the PLL is assumed as:

$$v_{in}(t) = \hat{V}\sin(\omega_0 t \;+\; \Delta\theta) \tag{3}$$

where $\Delta\theta$ represents small perturbation in the input signal. From Fig. 2, it is observed that there are four states in the system x_1-x_4 and the output y is considered as $\Delta\omega$. The LTP small signal state-space model is derived using two interconnected modules: 1) LTP model for SOGI and 2) LTP model for SRF-PLL. The two models obtained are then connected as shown in Fig. 3. Compared to the derivation approach which deals with the entire system, this derivation and modeling approach reduces the time for debugging, and makes the model easier to analyze.

A. LTP Model of SOGI

The SOGI has two states $x_3(t)$ and $x_4(t)$, with input $v_\alpha(t)$ and $\dot{x}_2(t)$. According to Fig. 2 block diagram of SOGI-PLL, the differential equations for the two states are:

$$\begin{aligned} \dot{x_3}(t) &= \left(\sqrt{2}\, v_{in}(t) - \sqrt{2}\, x_3(t) - \; x_4(t)\right)\; \dot{x_2}(t) \\ &= \left(\sqrt{2}\, v_{in}(t) - \sqrt{2}\, x_3(t) - \; x_4(t)\right)\; y(t) \\ \dot{x_4}(t) &= x_3(t)\; \dot{x_2}(t) = x_3(t) y(t) \end{aligned} \tag{4}$$

where $y = \dot{x_2}$ at steady-state is ω_0.

Now, states ($x_3(t)$ and x_4(t)) are assumed to have a small deviation from the steady state operating trajectories, given as:

$$\begin{aligned} x_3(t) &= x_{30}(t) + \Delta x_3(t) \\ x_4(t) &= x_{40}(t) + \Delta x_4(t) \end{aligned} \tag{5}$$

where x_{30} and x_{40} are steady state operating trajectories for the two states, and are given by $\hat{V}\;\sin(\omega_0\, t + \theta)$ and $\hat{V}\;\sin(\omega_0\, t + \theta - 90°)$ respectively, and Δx_3 and Δx_4 are the small deviations. $\hat{V}$ is assumed to be 1 and the initial angle θ_0 is assumed to be 0. Using, (5) in (4) the small-signal state-space model is obtained, and is provided in the matrix form in (6).

$$\begin{bmatrix} \Delta\,\dot{x_3}(t) \\ \Delta\dot{x_4}(t) \end{bmatrix} = \overbrace{\begin{bmatrix} -\sqrt{2}\omega_0 & -\omega_0 \\ \omega_0 & 0 \end{bmatrix}}^{A_2(t)} \overbrace{\begin{bmatrix} \Delta x_3(t) \\ \Delta x_4(t) \end{bmatrix}}^{\Delta x_b(t)} + \overbrace{\begin{bmatrix} \sqrt{2}\,\omega_0\cos(\omega_0 t) & \cos(\omega_0 t) \\ 0 & \sin(\omega_0 t) \end{bmatrix}}^{B_2(t)} \overbrace{\begin{bmatrix} \Delta\theta(t) \\ \Delta y(t) \end{bmatrix}}^{\Delta u_b(t)} \tag{6}$$

From (6) it is observed that matrix $B_2(t)$ is time-periodic in nature, with a time period of T_0 (= $2\pi/\omega_0$).

B. LTP Model for SRF-PLL

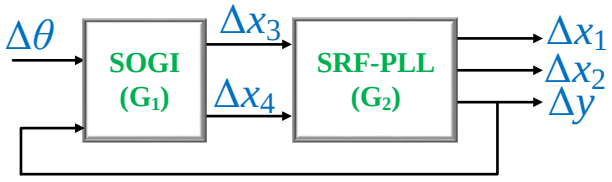

Fig. 3: Simplified block-by-block representation of the SOGI-PLL, adopted for modeling.

In the similar fashion, SRF-PLL has two states $x_1(t)$ and $x_2(t)$, with input $x_3(t)$ and $x_4(t)$. The differential equations for the two states and output variable (y) are:

$$\begin{aligned} \dot{x_1}(t) &= k_i\; v_q(t) \\ \dot{x_2}(t) &= \omega_0 + x_1(t) + k_p\; v_q(t) \\ \Delta\omega(t) &= y = x_1(t) + k_p\; v_q(t) \end{aligned} \tag{7}$$

where v_q is the q-axis component obtained from the Park's transformation, is given by :

$$v_q(t) = \cos(x_2)\, x_3 + \sin(x_2)\, x_4 \tag{8}$$

Using Taylor's series expansion on (8) we get:

$$\Delta v_q(t) = -\Delta x_2 + \cos(\omega_0\, t)\, \Delta x_3 + \sin(\omega_0\, t)\, \Delta x_4 \tag{9}$$

with the help of (9), (7) can be transformed to small signal state-space model, and is presented in the matrix format as:

$$\begin{bmatrix} \Delta \dot{x_1}(t) \\ \Delta \dot{x_2}(t) \end{bmatrix} = \overbrace{\begin{bmatrix} -0 & -k_i \\ 1 & -k_p \end{bmatrix}}^{A_1(t)} \overbrace{\begin{bmatrix} \Delta x_1(t) \\ \Delta x_2(t) \end{bmatrix}}^{\Delta x_a(t)} + \overbrace{\begin{bmatrix} k_i \cos(\omega_0 t) & k_i \sin(\omega_0 t) \\ k_p \cos(\omega_0 t) & k_p \sin(\omega_0 t) \end{bmatrix}}^{B_1(t)} \overbrace{\begin{bmatrix} \Delta x_3(t) \\ \Delta x_4(t) \end{bmatrix}}^{\Delta u_a(t)} \tag{10}$$

$$\Delta y(t) = \overbrace{\begin{bmatrix} 1 & -k_p \end{bmatrix}}^{C_1(t)} \begin{bmatrix} \Delta x_1(t) \\ \Delta x_2(t) \end{bmatrix} + \overbrace{\begin{bmatrix} k_p\, \cos(\omega_0\, t) & k_p\, \sin(\omega_0\, t) \end{bmatrix}}^{D_1(t)} \begin{bmatrix} \Delta x_3(t) \\ \Delta x_4(t) \end{bmatrix} \tag{11}$$

From (10) and (11) it is observed that matrix $B_1(t)$ and $D_1(t)$ are time-periodic in nature, with a time period of T_0.

IV. LTI Modeling of SOGI-PLL

Next step is to formulate the LTI model from the periodic state-space model obtained in (6), (10), and (11). The Harmonic Balance, proposed by Hill [11] back in 1886, is implemented to map the LTP system to the LTI system. The Harmonic balance refers to expansion of the time-periodic quantities using complex Fourier series. The time-domain signals $x_a(t)$, $x_b(t)$and $\Delta y(t)$ are expanded using complex Fourier series and "*exponentially modulated periodic* (EMP) " signal.

In this paper, the time-periodic quantities are assumed to have three frequency components, $\pm$ 60 Hz and 0 Hz. For instance, the time-periodic matrix $A_1(t)$ can be represented as:

$$A_1(t) = A_{1,0} + A_{1,1}\, e^{j\omega_0 t} + A_{1,-1}\, e^{-j\omega_0 t} \tag{12}$$

Here, $A_{1,0}$, $A_{1,1}$ and $A_{1,-1}$ are the complex Fourier coefficient of time-periodic matrix A_1 for 0 Hz, and $\pm$ 60 Hz respectively. It should be noted that, the complex Fourier coefficient are in fact time-invariant in nature. In the similar fashion, other matrices $A_2(t)$, $B_1(t)$, $B_2(t)$, $C_1(t)$ and $D_1(t)$ are expanded.

Now, the time-periodic state variables matrix $\Delta x_a(t)$, is expanded using complex Fourier series and EMP signal:

$$e^{st}\Delta x_a(t) = X_{a,0}\, e^{st} + X_{a,1}\, e^{(s+j\omega_0)t} + X_{a,-1}\, e^{(s-j\omega_0)t} \tag{13}$$

where $X_{a,0}$, $X_{a,1}$ and $X_{a,-1}$ are the complex Fourier coefficient of time-periodic signal $\Delta x_a(t)$ for 0 Hz, and $\pm$ 60 Hz respectively. In the similar way, other signals and state-variables $\Delta x_b(t)$, $\Delta\theta(t)$, and $\Delta y(t)$ are also expanded.

A. LTI Model of SOGI

Using the concept developed earlier from (12) and (13), in (6), the LTI model for SOGI can be obtained as shown:

$$s \begin{bmatrix} X_{b,-1} \\ X_{b,0} \\ X_{b,1} \end{bmatrix} = \left(\overbrace{\begin{bmatrix} A_{2,0} & A_{2,-1} & 0 \\ A_{2,1} & A_{2,0} & A_{2,-1} \\ 0 & A_{2,1} & A_{2,0} \end{bmatrix}}^{\mathbf{A}_2} - diag \overbrace{\begin{bmatrix} -j\omega_0 \\ 0 \\ j\omega_0 \end{bmatrix}}^{\mathbf{N}} \right) \times \overbrace{\begin{bmatrix} X_{b,-1} \\ X_{b,0} \\ X_{b,1} \end{bmatrix}}^{\mathbf{X}_b} + \overbrace{\begin{bmatrix} B_{2,0} & B_{2,-1} & 0 \\ B_{2,1} & B_{2,0} & B_{2,-1} \\ 0 & B_{2,1} & B_{2,0} \end{bmatrix}}^{\mathbf{B}_2} \overbrace{\begin{bmatrix} U_{b,-1} \\ U_{b,0} \\ U_{b,1} \end{bmatrix}}^{\mathbf{U}_b} \tag{14}$$

Equation (14) represents the LTI model obtained from the LTP state-space model. It should be noted that matrices $\mathbf{A}_2$, and $\mathbf{B}_2$ contains the complex Fourier coefficients for matrix $A_2(t)$ and $B_2(t)$, and are time-invariant in nature. Matrix $\mathbf{N}$ is a diagonal matrix containing the information about the harmonic frequencies present in the system. $\mathbf{U}_b$ is a time-invariant matrix containing the complex Fourier coefficients of the input to SOGI block i.e., $\Delta\theta$ and Δy.

B. LTI Model of SRF-PLL

On the similar lines as of SOGI block, the LTI model of the SRF-PLL is derived from (10), and (11) is given by:

$$s \begin{bmatrix} X_{a,-1} \\ X_{a,0} \\ X_{a,1} \end{bmatrix} = \left(\overbrace{\begin{bmatrix} A_{1,0} & A_{1,-1} & 0 \\ A_{1,1} & A_{1,0} & A_{1,-1} \\ 0 & A_{1,1} & A_{1,0} \end{bmatrix}}^{\mathbf{A}_1} - diag \overbrace{\begin{bmatrix} -j\omega_0 \\ 0 \\ j\omega_0 \end{bmatrix}}^{\mathbf{N}} \right) \times \overbrace{\begin{bmatrix} X_{a,} \\ X_{a,0} \\ X_{a,1} \end{bmatrix}}^{\mathbf{X}_a} + \overbrace{\begin{bmatrix} B_{1,0} & B_{1,-1} & 0 \\ B_{1,1} & B_{1,0} & B_{1,-1} \\ 0 & B_{1,1} & B_{1,0} \end{bmatrix}}^{\mathbf{B}_1} \overbrace{\begin{bmatrix} U_{a,-1} \\ U_{a,0} \\ U_{a,1} \end{bmatrix}}^{\mathbf{U}_a} \tag{15}$$

$$\begin{bmatrix} Y_{-1} \\ Y_0 \\ Y_1 \end{bmatrix} = \overbrace{\begin{bmatrix} C_{1,0} & C_{1,-1} & 0 \\ C_{1,1} & C_{1,0} & C_{1,-1} \\ 0 & C_{1,1} & C_{1,0} \end{bmatrix}}^{\mathbf{C}_1} \times \overbrace{\begin{bmatrix} X_{-1} \\ X_0 \\ X_1 \end{bmatrix}}^{\mathbf{X}_a} + \overbrace{\begin{bmatrix} D_{1,0} & D_{1,-1} & 0 \\ D_{1,1} & D_{1,0} & D_{1,-1} \\ 0 & D_{1,1} & D_0 \end{bmatrix}}^{\mathbf{D}_1} \overbrace{\begin{bmatrix} U_{a,-1} \\ U_{a,0} \\ U_{a,1} \end{bmatrix}}^{\mathbf{U}_a} \tag{16}$$

$\mathbf{U}_a$ is a time-invariant matrix containing the complex Fourier coefficients of the input to SRF-PLL block i.e., Δx_3 and Δx_4.

In summary, the LTP model obtained in Section III for SOGI and SRF-PLL is mapped to a LTI model using the complex Fourier series expansion, and are presented in (14), (15) and (16). The two separate LTI models (SOGI, and SRF-PLL) are connected in the similar way as depicted in Fig. 3.

To obtain the value of complex Fourier coefficients for periodic matrices $A_1(t)$, $B_1(t)$, $C_1(t)$, $D_1(t)$, $A_2(t)$ and

$B_2(t)$, Euler's identity of sine and cosine is used. For instance, from (6) $B_2(t)$ is expressed as:

$$B_2(t) = \overbrace{\begin{bmatrix} 0 & 0 \\ 0 & 0 \end{bmatrix}}^{B_{2,0}} + \overbrace{\begin{bmatrix} \sqrt{2}\omega_0/2 & 1/2 \\ 0 & 1/(2j) \end{bmatrix}}^{B_{2,1}} e^{j\omega_0 t} + \overbrace{\begin{bmatrix} \sqrt{2}\omega_0/2 & 1/2 \\ 0 & -1/(2j) \end{bmatrix}}^{B_{2,-1}} e^{-j\omega_0 t} \tag{17}$$

V. Simulations

The two models obtained, i.e., the LTP model and the LTI model, are simulated in MATLAB / Simulink environment, and bench-marked with the nonlinear model of the SOGI-PLL (Fig. 2). The parameters for the PI controller's gains k_p and k_i are 60 and 1400 respectively, and the fundamental frequency ω_0 is 377 rad/s. The magnitude of input signal $\hat{V}$ is 1 $p.u.$ A step change is applied to the input u (= $\Delta\theta$) at t = 0.5s of 10°.

A. Simulation results from the LTP Model

The outputs from the LTP model are the time-domain signals. The step response is shown in Fig. 4, in which the time-domain results are presented for the LTP model and the nonlinear model of the SOGI-PLL. It is observed from Fig. 4 that the results from the LTP model and nonlinear model match exactly.

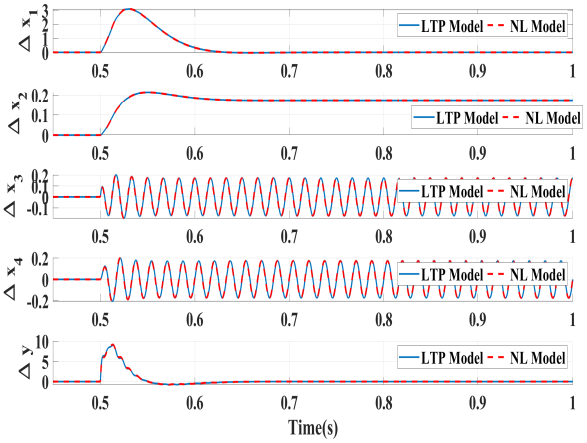

Fig. 4: Performance of the LTP Model compared to the nonlinear (NL) model, when a phase jump of 10° is introduced.

B. Simulation results from LTI Model

The outputs from the LTI model presented in (14) and (15) and (16) are the complex Fourier coefficients for various time domain periodic signals, which are time-invariant in nature. The input $\Delta\theta$ has three frequency components as defined in Section V. For analysis and validations, a step change of 10°(=0.1745 radians) at t = 0.5s is applied to the 0 Hz component of the input. The absolute values of the complex Fourier coefficients are present in Fig. 5.

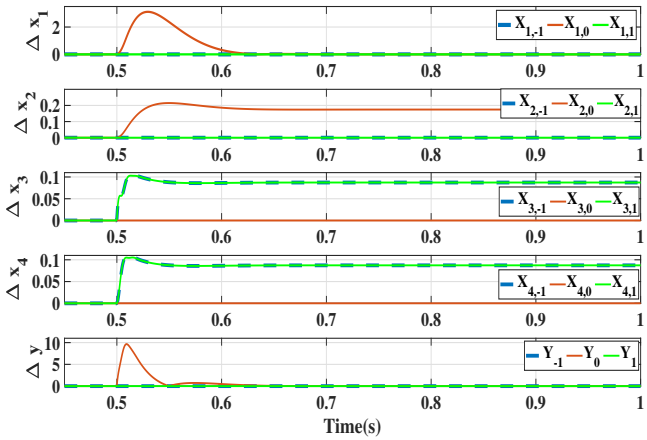

Fig. 5: Absolute value of the complex Fourier coefficients of Δx_1 - Δx_4 and Δy, obtained from the LTI model after a step change of 10 ° in the DC component of input $\Delta\theta$ is applied.

Now, the objective is to recreate the time-domain signal, so as to validate the derived LTI model with the nonlinear model. The complex Fourier coefficients obtained from the LTI model are represented in phasor domain and are then used to re-construct the time-domain signals $\Delta x_1(t)$–$\Delta x_4(t)$ and $\Delta y(t)$. For example $\Delta x_1(t)$, is represented as:

$$\Delta x_1(t) = \text{Real}\left[|X_{1,0}|e^{j\theta_{1,0}} + |X_{1,1}|e^{j\theta_{1,1}}e^{j\omega_0 t} + |X_{1,-1}|e^{j\theta_{1,-1}}e^{-j\omega_0 t}\right] \tag{18}$$

where $|X_{1,0}|$, $|X_{1,1}|$ and $|X_{1,-1}|$ are the absolute values (Fig. 5), and $\theta_{1,0}$, $\theta_{1,1}$ and $\theta_{1,-1}$ are the phase angles of complex Fourier coefficients for Δx_1 for 0 Hz and ±60 Hz respectively. In the similar way, other signals are also obtained.

The comparison between the reconstructed signal from the LTI model and the nonlinear model is presented in Fig. 6, when a step change of 10° is applied to the 0 Hz component of the input at t = 0.5s. The results demonstrate that the dervied LTI model and nonlinear model corroborate each other.

Remarks: Fig. 4 represents the comparison between the results obtained from the LTP model and the nonlinear model. The outputs from the LTP model are the time-domain signals. In Fig. 5 the absolute value complex Fourier coefficients for $\Delta x_1(t)$–$\Delta x_4(t)$ and $\Delta y(t)$ are presented. With the help of complex Fourier coefficients, the time domain signals are recreated and are compared with the nonlinear model for validation of the LTI model. The results are shown in Fig. 6.

C. Validation of the LTI model using Bode Plots

Harmonic injection or frequency scanning methodology is a popular technique to obtain input-output relationship in frequency domain [12]. To further validate LTI model,

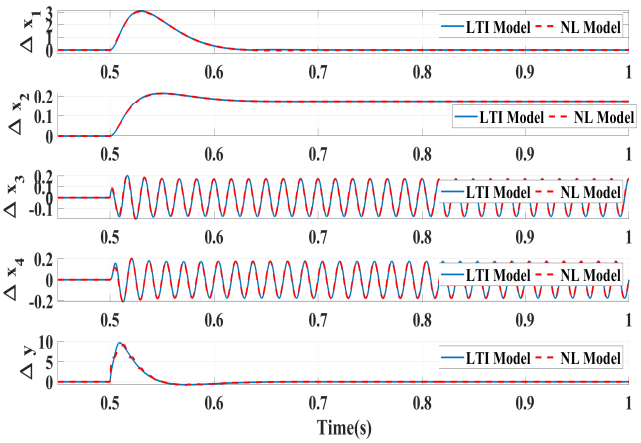

Fig. 6: Comparison of the re-constructed time-domain signal from the complex Fourier coefficients obtained from the LTI model with the time signal from the nonlinear (NL) model.

harmonic perturbation is applied to DC component of $\Delta\theta$ in the nonlinear model. The perturbation is given as:

$$\Delta\theta_p(t) = \hat{\theta_p}\cos(2\pi f_p t) \tag{19}$$

where $\hat{\theta_p}$ is the magnitude of perturbation and is equal to 0.01 radians. Perturbation frequency is represented by f_p, and its range is from 1 Hz to 150 Hz, with a step size of 1Hz.
For each injected frequency, time domain data for $\Delta\omega$ is recorded. Fast Furious Transform (FFT) algorithm is performed on the recorded time domain data, to extract magnitude and phase at the same injected frequency. The transfer function is then formed as:

$$G(f_p) = \frac{\Delta\omega(f_p)}{\Delta\theta_p(f_p)} \tag{20}$$

In the LTI model, MATLAB command "*linmod*" is used to obtain transfer function between the DC component of the input $\Delta\theta$ and the complex Fourier coefficient of $\Delta\omega$ for 0 Hz component. The Bode plots of transfer function obtained from harmonic injection method (20), and from the LTI model are presented in Fig. 7. It is observed from Fig. 7, both the transfer functions are a good match. This further validates the derived LTI model.

VI. Conclusion

In this paper, the concept of Harmonic State Space modeling is adopted to model SOGI-PLL. First, the LTP model is mathematically derived by linearzing the nonlinear system at steady-state periodic trajectory. From the LTP model obtained, harmonic balance or harmonic linearization method is used to obtain the LTI model. For the LTI model, only relevant harmonics are used to represent the system. For modeling process, block by block approach is adopted. The performance of the two models was compared with the nonlinear model of SOGI-PLL, when a phase jump is applied to the initial phase angle of the input signal. Bode plots of the transfer functions

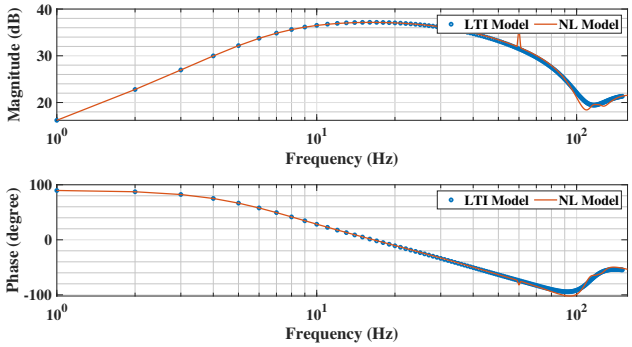

Fig. 7: Comparison of the transfer function obtained from the LTI model and from the nonlinear model (harmonic perturbation), between the DC component of $\Delta\theta$ and $\Delta\omega$.

obtained from the LTI model, and the nonlinear model are also presented for further validation. All the simulations are done using MATLAB/Simulink environment.

References

[1] S. Golestan, J. M. Guerrero, and J. C. Vasquez, "Single-phase PLLs: A review of recent advances," *IEEE Transactions on Power Electronics*, vol. 32, no. 12, pp. 9013–9030, 2017.

[2] Y. Han, M. Luo, X. Zhao, J. M. Guerrero, and L. Xu, "Comparative performance evaluation of orthogonal-signal-generators-based single-phase pll algorithms—a survey," *IEEE Transactions on Power Electronics*, vol. 31, no. 5, pp. 3932–3944, 2016.

[3] R. Teodorescu, M. Liserre, and P. Rodriguez, *Grid converters for photovoltaic and wind power systems*. John Wiley & Sons, 2011, vol. 29.

[4] R. M. Santos Filho, P. F. Seixas, P. C. Cortizo, L. A. B. Torres, and A. F. Souza, "Comparison of three single-phase PLL algorithms for ups applications," *IEEE Transactions on Industrial Electronics*, vol. 55, no. 8, pp. 2923–2932, 2008.

[5] S. Golestan, M. Monfared, F. D. Freijedo, and J. M. Guerrero, "Dynamics assessment of advanced single-phase PLL structures," *IEEE Transactions on Industrial Electronics*, vol. 60, no. 6, pp. 2167–2177, 2013.

[6] F. Xiao, L. Dong, L. Li, and X. Liao, "A frequency-fixed SOGI-based PLL for single-phase grid-connected converters," *IEEE Transactions on Power Electronics*, vol. 32, 2017.

[7] N. M. Wereley, "Analysis and control of linear periodically time varying systems," Ph.D. dissertation, Massachusetts Institute of Technology, 1990.

[8] J. R. C. Orillaza and A. R. Wood, "Harmonic state-space model of a controlled TCR," *IEEE Transactions on Power Delivery*, vol. 28, no. 1, pp. 197–205, 2013.

[9] S. Golestan, J. M. Guerrero, and J. C. Vasquez, "Modeling and stability assessment of single-phase grid synchronization techniques: Linear time-periodic versus linear time-invariant frameworks," *IEEE Transactions on Power Electronics*, vol. 34, no. 1, pp. 20–27, 2019.

[10] M. Ciobotaru, R. Teodorescu, and F. Blaabjerg, "A new single-phase PLL structure based on second order generalized integrator," in *2006 37th IEEE Power Electronics Specialists Conference*, 2006, pp. 1–6.

[11] G. W. Hill *et al.*, "On the part of the motion of the lunar perigee which is a function of the mean motions of the sun and moon," *Acta mathematica*, vol. 8, pp. 1–36, 1886.

[12] B. Badrzadeh, M. Sahni, Y. Zhou, D. Muthumuni, and A. Gole, "General methodology for analysis of sub-synchronous interaction in wind power plants," *IEEE Transactions on Power Systems*, vol. 28, no. 2, pp. 1858–1869, 2013.